Electronic Supplementary Material (ESI) for Nanoscale.

On-Surface Porphyrin Transmetalation with Pb/Cu Redox Exchange

Jan Herritsch, Stefan R. Kachel, Qitang Fan, Mark Hutter, Lukas J. Heuplick, Florian Münster, J. Michael Gottfried*

Department of Chemistry, Philipps University of Marburg, Hans-Meerwein-Straße 4, 35032 Marburg, Germany, michael.gottfried@chemie.uni-marburg.de

Table of Contents

1 PbTPP Multilayer Spectra and Purity of the Deposited Films

In addition to the information about the electronic structure of the surface-decoupled PbTPP molecules, multilayer spectra can be used to evaluate the purity of the deposited films. In particular, a contamination by the free-base ligand 2HTPP is critical. The unmetalated porphyrin 2HTPP does react with the Cu(111) in an on-surface self-metalation at 420−450 K forming CuTPP.[1-5] Therefore, if such an 2HTPP impurity is present in the studied PbTPP films, the detection of CuTPP in the TPR experiment can no longer be attributed solely to the transmetalation of type PbTPP + Cu → CuTPP + Pb. The unmetalated porphyrin 2HTPP could be easily identified by XPS because it exhibits two pyrrolic (−NH−) and two iminic (−N=) nitrogen atoms and consequently there is a splitting of the N 1s signal. In contrast to this, the measured N 1s consists only of a single narrow peak indicating that all nitrogen atoms are equivalent (N−Pb). Thus, it can be concluded that there are no significant contaminations by 2HTPP. Moreover, the Pb 4f signal corresponds to the typical shape of lead(II) tetrapyrroles.[6-9]

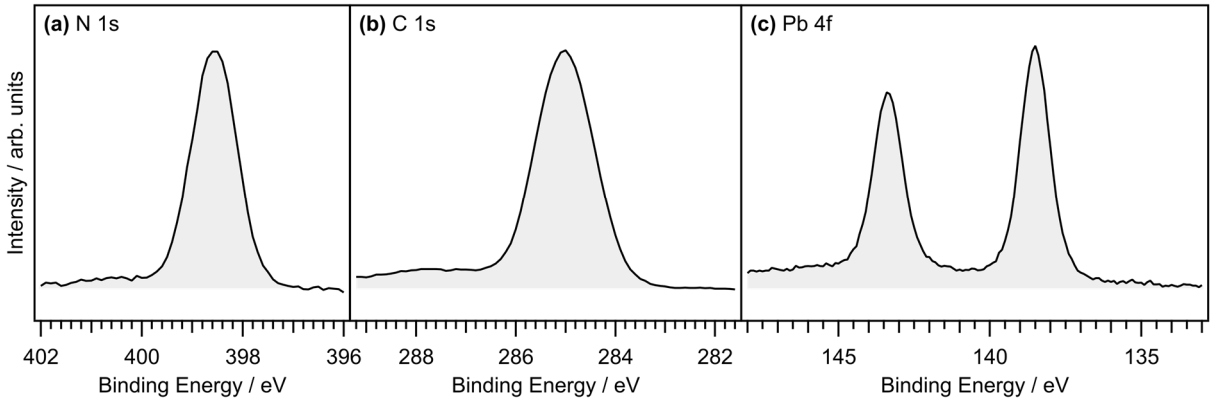

Figure S1. XP spectra of the PbTPP multilayer of 4.0 nm thickness deposited on the Cu(111) substrate for (a) the N 1s, (b) C1s, and (c) Pb 4f region. For a simple representation, the intensity was scaled differently for the individual regions.

2 Detailed Temperature Series of a PbTPP Monolayer on Cu(111)

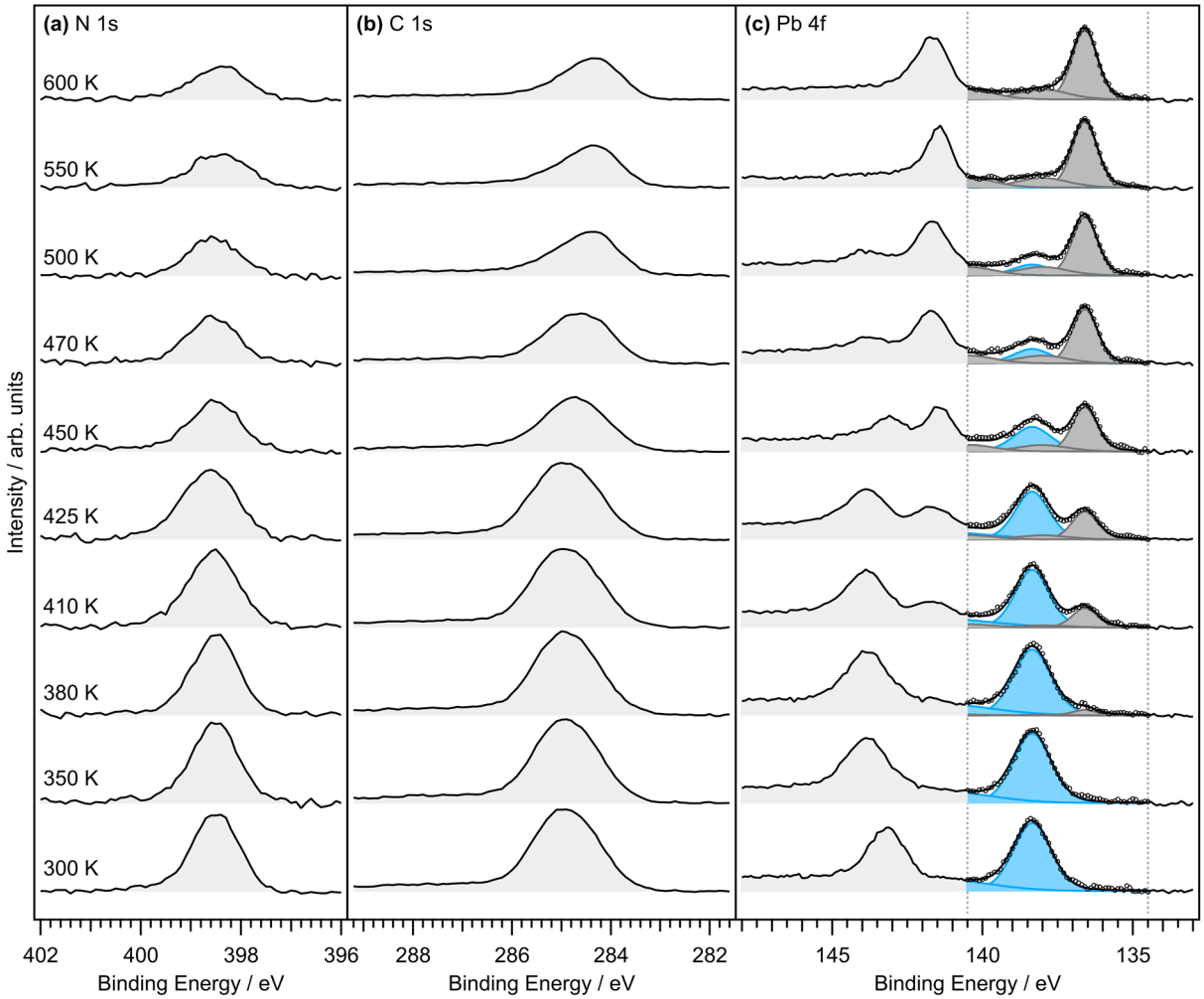

Figure S2. XPS series of a monolayer PbTPP on Cu(111) for (a) the N 1s, (b) the C 1s, and (c) the Pb 4f region. Spectra were measured at 300 K after annealing the sample for 3 min at the indicated temperatures. The Pb $4f_{7/2}$ region between 134.5 eV and 140.5 eV is described by a fit of the Pb(II) (coloured in blue) and the Pb(0) (coloured in grey) moieties. Here, the black line is the sum of both components while open circles represent the experimental data. For a simple representation, the intensity was scaled differently for the individual regions.

3 Island Conformer at Higher Coverages (>0.25 ML)

At low submonolayer coverages (0.25 ML), the molecules are separated and do not aggregate. They appear rectangular shape (see discussion in the manuscript). However, increasing the coverage (0.40 ML) the molecules start to form islands, which are shown in Figure S3a,b. In this islands PbTPP is densely packed and adopts a square shape. Moreover, the peripheral substituents are protruding which can be explained by a rotation of the phenyl rings. Thus, the upright standing substituents enable the formation of T-shaped π stacking interaction, because the phenyl rings point towards the centre of the neighbouring molecule's phenyl ring. Figure S3c shows the proposed molecular structure of the island conformer in comparison with the single molecule conformer. The islands are not stable at higher temperatures and disappear completely after annealing the sample to 450 K (Figure S4). This process might be associated with the partial desorption of the monolayer.

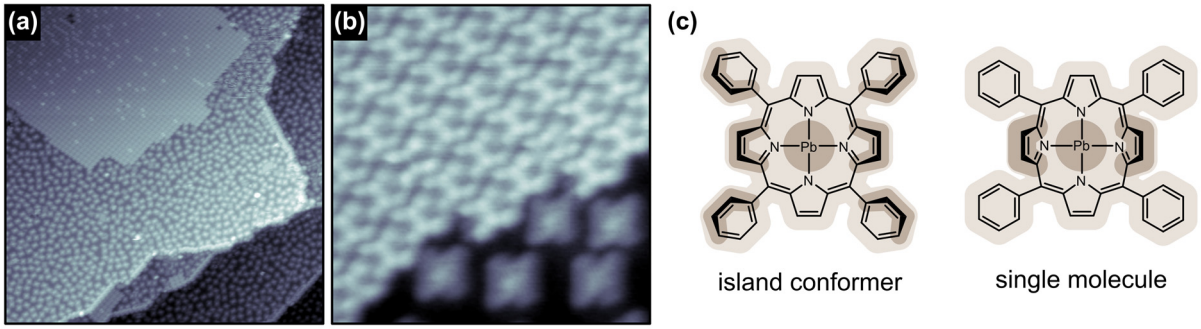

Figure S3. STM images of (a,b) a PbTPP submonolayer (0.40 ML) on Cu(111); (c) proposed molecular structures for the island conformer compared to the single molecule or inverted conformer, which is discussed in the manuscript in detail. The shading highlights protruding parts. Tunneling parameters: (a) $U = -0.27$ V, $I = -0.02$ nA, 100.0×100.0 nm^2; (b) $U = -0.27$ V, $I = -0.03$ nA, 10.0×10.0 nm^2.

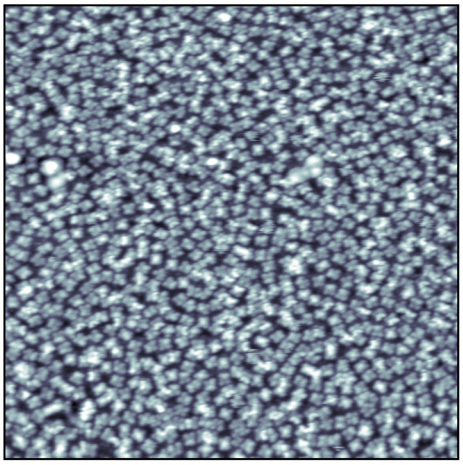

Figure S4. STM image of the same sample (0.40 ML) after annealing to 450 K. The island conformer has completely disappeared and partial dehydrogenation of the peripheral phenyl substituents has started. Tunneling parameters: $U = +1.63$ V, $I = +0.02$ nA, 70.0×70.0 nm^2.

4 Progress of On-Surface Transmetalation (Monolayer versus Submonolayer)

The temperature-dependent progress for the transmetalation can be derived from the XPS heating series with the fitted Pb 4f region. The Cu-Pb exchange is obtained directly from the ratio of the Pb(II) and the Pb(0) signal intensities *I*.

$$\text{exchange(XPS)} = \frac{I_{\text{Pb(0)}}}{I_{\text{Pb(0)}} + I_{\text{Pb(II)}}} \times 100$$

Alternatively, it can be estimated using STM images by counting the number of molecules, $n_{\text{molecules}}$, and the number of visible Pb(0) atoms, $n_{\text{Pb(0)}}$, assuming that the difference between $n_{\text{molecules}}$ and $n_{\text{Pb(0)}}$ is equal to the number of molecules containing Pb(II), $n_{\text{Pb(II)}}$.

$$\text{exchange(STM)} = \frac{n_{\text{Pb(0)}}}{n_{\text{Pb(0)}} + n_{\text{Pb(II)}}} \times 100 = \frac{n_{\text{Pb(0)}}}{n_{\text{Pb(0)}} + (n_{\text{molecules}} - n_{\text{Pb(0)}})} \times 100 = \frac{n_{\text{Pb(0)}}}{n_{\text{molecules}}} \times 100$$

In Table S1, the resulting values for the submonolayer sample (0.25 ML) are compared. There is a good agreement of the Pb−Cu exchange obtained by XPS with STM.

Table S1. Results for the progress of the on-surface transmetalation plotted in Figure 6.

temperature / K	$n_{\text{molecules}}$	$n_{\text{Pb(0)}}$	exchange (STM)	exchange (XPS)
300	65	1	2%	0%
450	60	32	53%	47%
550	62	59	95%	94%

5 STM Images with Increased Brightness and Contrast

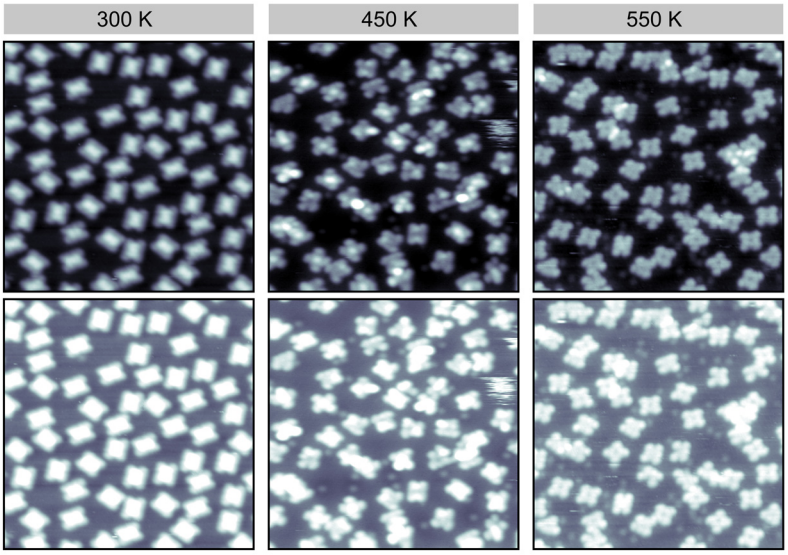

Figure S5. Upper panels: STM images of a submonolayer PbTPP on Cu(111) (from Figure 5 in the manuscript). Lower panels: The same STM images, but with increased contrast and brightness, resulting in better visibility of the individual Pb(0) atoms.

6 References

1. Y. Xiao, S. Ditze, M. Chen, F. Buchner, M. Stark, M. Drost, H.-P. Steinrück, J. M. Gottfried and H. Marbach, *J. Phys. Chem. C*, 2012, **116**, 12275-12282.
2. K. Diller, F. Klappenberger, M. Marschall, K. Hermann, A. Nefedov, C. Wöll and J. V. Barth, *J. Chem. Phys.*, 2012, **136**, *136*, 014705.
3. M. Röckert, M. Franke, Q. Tariq, D. Lungerich, N. Jux, M. Stark, A. Kaftan, S. Ditze, H. Marbach, M. Laurin, J. Libuda, H.-P. Steinrück and O. Lytken, *J. Phys. Chem. C*, 2014, **118**, 26729-26736.
4. M. Röckert, M. Franke, Q. Tariq, S. Ditze, M. Stark, P. Uffinger, D. Wechsler, U. Singh, J. Xiao, H. Marbach, H.-P. Steinrück and O. Lytken, *Chem. Eur. J.*, 2014, **20**, 8948-8953.
5. M. Röckert, S. Ditze, M. Stark, J. Xiao, H.-P. Steinrück, H. Marbach and O. Lytken, *J. Phys. Chem. C*, 2014, **118**, 1661-1667.
6. A. Rager, B. Gompf, L. Dürselen, H. Mockert, D. Schmeisser and W. Göpel, *J. Mol. Electron.*, 1989, **5**, 227-238.
7. L. Ottaviano, L. Lozzi, S. Santucci, S. D. Nardo and M. Passacantando, *Surf. Sci.*, 1997, **392**, 52-61.
8. N. Papageorgiou, J. C. Mossoyan, M. Mossoyan-Deneux, G. Terzian, E. Janin, M. Göthelid, L. Giovanelli, J. M. Layet and G. L. Lay, *Appl. Surf. Sci.*, 2000, **162-163**, 178-183.
9. J. D. Baran, J. A. Larsson, R. A. J. Woodley, Y. Cong, P. J. Moriarty, A. A. Cafolla, K. Schulte and V. R. Dhanak, *Phys. Rev. B*, 2010, **81**, 075413.